

Theoretical study on the reaction of hydrogen atoms with aniline

Marwan Batiha · Mohammednoor Altarawneh ·
Abdullah Alsofi · Mohammad Al-Harahsheh ·
Ibrahem Altarawneh · Saleh Alrawadieh

Received: 2 February 2011 / Accepted: 5 April 2011 / Published online: 23 April 2011
© Springer-Verlag 2011

Abstract The reaction of aniline with hydrogen atom is investigated herein using the hybrid meta-DFT functional of BB1 K. Hydrogen atom is found to preferentially add at an *ortho* position. However, the fate of the *o*-(C₆H₅NH₂)H adduct is found to be solely the deactivation of the initial addition channel. The rate constant for the abstraction channel (C₆H₅NH₂ + H → C₆H₅NH + H₂) is fitted by the expression 1.10 × 10⁻¹¹ exp(-4,200/T) cm³ molecule⁻¹ s⁻¹. Our calculated rate constant for the abstraction channel agrees very well with the available experimental measurements. Satisfactory agreement is found between calculated and experimental measurements for the displacement channel (C₆H₅NH₂ + H → C₆H₆ + NH₂). Our detailed analysis for the corresponding displacements in toluene and phenol suggests that the three systems exhibit similar behavior with regard to the relative importance of abstraction and displacement channels.

Keywords Aniline · Hybrid meta-DFT · Reaction rate constant · Abstraction vs. displacement · H atoms

Electronic supplementary material The online version of this article (doi:[10.1007/s00214-011-0940-x](https://doi.org/10.1007/s00214-011-0940-x)) contains supplementary material, which is available to authorized users.

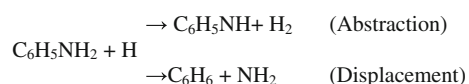
M. Batiha · M. Altarawneh (✉) · A. Alsofi ·
I. Altarawneh · S. Alrawadieh
Department of Chemical Engineering,
Al-Hussein Bin Talal University, Ma'an, Jordan
e-mail: mn.Alt@ahu.edu.jo

M. Al-Harahsheh
Department of Mining Engineering,
Al-Hussein Bin Talal University, Ma'an, Jordan

1 Introduction

Aniline or aminobenzene (C₆H₅NH₂) is an important precursor in various chemical industries, including the manufacturing of rubbers, explosions, and fertilizers. It is also used in petroleum refinery [1]. Aniline is regarded as notorious organic pollutant. It has adverse effect on human health as well as on the environment; especially aquatic life [2]. Aniline inventory is predominantly man-made, yet there is also a significant contribution from forest fires. Most aniline is deposited directly to the atmosphere and a small portion to the water resources. Aniline has been detected in a wide range of air samples, from tobacco smoke to the effluent of oil refineries [3]. For instance, aniline was detected from the flashing and smoldering combustion of natural and RDF wood [4]. Atmospheric aniline is decomposed mainly through its reaction with hydroxyl radicals where a very short lifetime of 2.3 h is reported by Atkinson et al. [5]. Most environmental research on aniline has targeted its removal from wastewater using various techniques including biodegradation [6] and adsorption [7] by selective substrate.

While kinetic data concerning the reactions of substituted benzene compounds such as phenol and toluene with radicals at higher temperatures have been thoroughly addressed, corresponding data for aniline are rather scarce. To the best of our knowledge, there is only one experimental measurement for the reaction of aniline with H atoms. He et al. [8] investigated abstraction/displacement mechanisms in aniline:



He et al. [8] found that the two processes have very similar rate constants. In spite of the differences in

electronic properties induced by the three distinct functional groups in phenol, toluene and aniline, namely hydroxyl, methyl, and amino, rate constants for the displacement channel in these three compounds were found to be very similar.

To this end, we address in this theoretical study reaction rate constants and mechanism for the reaction of aniline with H atom. Our calculated values are compared with those of the very limited available experimental data. Results presented herein are instrumental in a better understanding of the reactions governing the hydrogenolysis of aniline. Furthermore, our results for the system (aniline + H) could be extended to the more complex structurally related amine-containing pesticides.

2 Computational details

The Gaussian 03 [9] suite of programs is used to carry out all electronic structure calculations. Optimized geometries and harmonic vibrational frequencies have been calculated using the meta hybrid density functional theory (DFT) of BB1 K [10] with the 6-311 ++G(2d,p) basis set [11]. The BB1 K functional is characterized by the deployment of an HF exchange fraction along with the abstraction of kinetic energy density from Kohn–Sham orbitals [12]. The BB1 K functional has been shown to significantly outperform all hybrid DFT methods including B3LYP in determination of saddle-point geometries and barrier heights, especially for hydrogen transfer reactions. BB1 K method is found to produce energies and activation barriers in close agreement with those obtained with ab initio methods such as MP2 and the chemistry models methods such as G3MP2B3 [13]. In order to provide a benchmark for the accuracy of the BB1IK/6-311 ++G(2d,p) methodology, reaction and activation energies for selected reactions are calculated also with the composite method of G3B3. All energies are corrected with zero-point vibrational energies (ZPVE).

Analysis of the vibrational frequency is used to determine the nature of the located stationary points as either minima or transition states (TS) where first-order saddle points contain one and only one imaginary frequency along the reaction coordinate. All TS are connected to their reactants and products via carrying out intrinsic reaction coordinate calculations (IRC). Vibrational frequencies corresponding to internal rotations have been treated as hindered rotors. The implementation and the necessity for this treatment to obtain reliable thermochemical parameters are well documented [14]. Chemrate code [15] is used to derive entropies and heat capacities. Rate constants, $k(T)$, are derived by conventional transition state theory (TST) [16]. The transmission coefficient that accounts for the quantum tunneling corrections is calculated with the one-

dimensional Eckart functional [17]. Rate constants are fitted to modified Arrhenius parameters in the temperature region of 300 K to 2,000 K as $k(T) = AT^n \exp(-Ea/RT)$, where A is the pre-exponential A-factor and Ea is the calculated energy of activation. Rate constants are calculated using TheRate code [18]. TheRate code is available online free of charge at the CSEO resource (<http://www.cseo.net>).

3 Results and discussions

3.1 Optimized structures

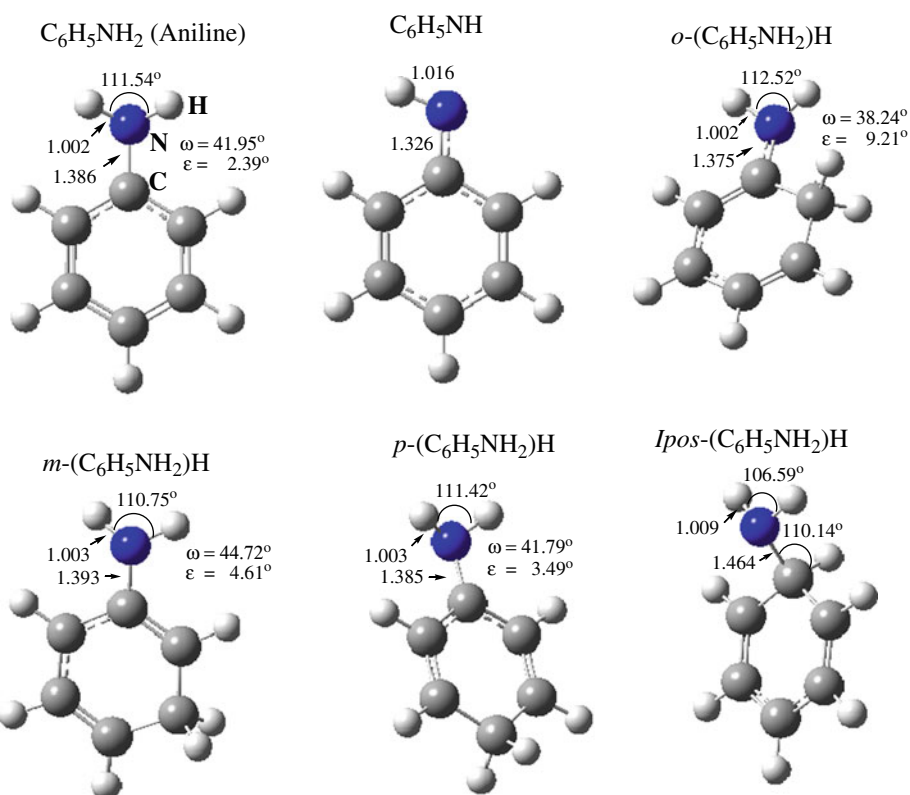
The structure of aniline has been studied both experimentally [19] and theoretically [20]. Most interest has been focused on measuring the pyramidalization of the amine group arising from asymmetric interaction between the amine group and the phenyl ring. The inversion (σ) and tilt (ϵ) angles are used as a measure of the degree of the pyramidalization, i.e., the deformation of the amine nitrogen from planarity. Various experimental measurements provide a value for the inversion angle between $37.48 \pm 2.0^\circ$ and $42.40 \pm 0.3^\circ$. As shown in the optimized structure of aniline in Fig. 1, our calculated inversion angle amount to 41.95° and is in close consensus with the experimental values. Other structural parameters including the tilt angle, the HNH angle, and bond lengths are also in good agreement with the experimental measurements.

Hydrogen atom reaction with aniline branches into four plausible addition sites as well as via the abstraction of one of the hydrogen atoms from the amine group. The four addition channels constitute the formation of *o*-(C₆H₅NH₂)H, *m*-(C₆H₅NH₂)H, *p*-(C₆H₅NH₂)H, and *ipso*-(C₆H₅NH₂)H adducts while the anilino radical (C₆H₅NH) is produced from the abstraction channel. Optimized structures are depicted in Fig. 1. The C–N bond in the anilino radical is shortened by 0.060 Å in reference to the aniline molecule. As can be seen in Fig. 1, the inversion and tilt angles in the *o*- and *p*-(C₆H₅NH₂)H adducts depart from the corresponding values in the aniline molecule; the difference is more profound in the *o*-(C₆H₅NH₂)H adduct. The *m*-(C₆H₅NH₂)H adduct exhibits to a large extent very similar geometrical features in reference to the aniline molecule.

3.2 Entropy and heat capacity

Torsional frequencies corresponding to the amine group in aniline *o*-(C₆H₅NH₂)H, *m*-(C₆H₅NH₂)H, *p*-(C₆H₅NH₂)H and *ipso*-(C₆H₅NH₂)H adducts were omitted from the calculations of $S^\circ(298.15\text{ K})$ and $Cp^\circ(T)$, and their contributions were replaced by hindered rotor contributions evaluated with their calculated rotational barriers,

Fig. 1 Optimized structures for aniline, anilino, and aniline-H adducts. Bond distances are in Å and angles are in degrees



symmetry numbers of rotation, and moment of inertia of the rotors. Rotational barriers and symmetry numbers of rotation were identified by performing partial optimization around the torsional angle at an interval of 30° at the B3LYP/6-31G(d) level of theory. Figure 2 depicts the internal rotational potential of the amine group in aniline. We attributed the presence of two additional minima in the energy potential in Fig. 2 to the interaction between rotation and inversion, i.e., the pyramidal NH_2 inverting through the planar form. The twofold rotational potentials shown in Fig. 2 has calculated barriers of $5.6 \text{ kcal mol}^{-1}$ and $1.4 \text{ kcal mol}^{-1}$, in relatively good agreement with the experimentally obtained values of $4.0 \text{ kcal mol}^{-1}$ and $1.4 \text{ kcal mol}^{-1}$ for the barriers for rotation and inversion in aniline using microwave spectroscopy [21]. One the other hand, the inversion barrier is also calculated by finding the energy difference between the C_{3v} and D_{3h} structures of aniline in view of the recently presented mythology for calculating barrier of inversion in ammonia by Halpern et al. [22]. The calculated difference between the C_{3v} and D_{3h} structures at the B3LYP/6-31G(d) level amounts to 1.2 kcal/mol , i.e., in good agreement with the experimental barrier of inversion.

The overall symmetry number is included in the calculations of $S^\circ(298.15 \text{ K})$ and $C_p^\circ(T)$. In our calculation for the entropy of aniline, only torsion of aniline is treated as hindered rotation while the inversion is treated as harmonic oscillator because the inversion mode is associated with a relatively large vibrational frequency, i.e., 623.459 cm^{-1} .

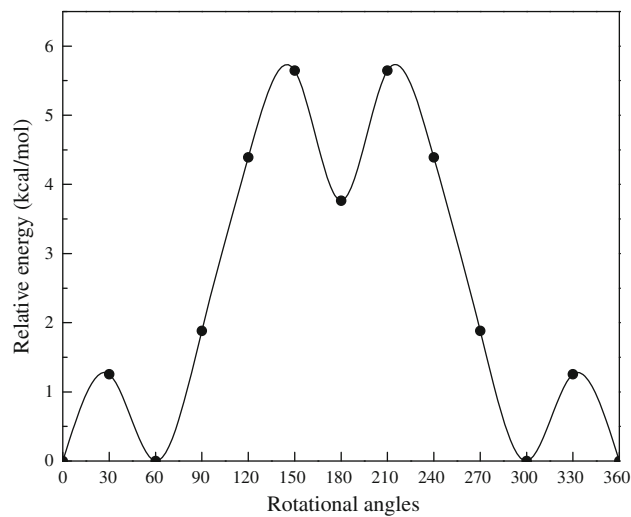


Fig. 2 Internal rotors potential for the amine group in aniline

Table 1 gives the calculated $S^\circ(298.15 \text{ K})$ and $C_p^\circ(T)$ values. A comparison is made with the limited available values for aniline [23]. Our calculated $S^\circ(298.15 \text{ K})$ value for aniline amounts to $75.31 \text{ cal K}^{-1} \text{ mol}^{-1}$ in very good agreement with the corresponding experimental value, i.e., $76.1 \text{ cal K}^{-1} \text{ mol}^{-1}$. It is worth mentioning that Hussein et al. [23] arrived theoretically to their experimental value; however, the deployed torsional vibrational frequency in their calculations frequency was 216 cm^{-1} calculated by

Table 1 S°_{298} and $C_p^\circ(T)$ in cal K $^{-1}$ mol $^{-1}$

	S°_{298}	$C_p^\circ(T)$				
		298.15 K	500 K	800 K	1,000 K	1,400 K
$C_6H_5NH_2$	75.31	25.31	40.65	53.97	59.35	66.17
$C_6H_5NH_2$ (exptl ^a)	76.10					
<i>o</i> -($C_6H_5NH_2$)H	80.06	27.53	43.66	57.86	63.70	71.14
<i>m</i> -($C_6H_5NH_2$)H	79.91	27.62	43.81	57.98	63.78	71.17
<i>p</i> -($C_6H_5NH_2$)H	81.00	27.68	43.69	57.87	63.71	77.13
<i>Ips</i> o-($C_6H_5NH_2$)H	80.41	26.92	43.39	57.76	63.68	77.11
C_6H_5NH	76.80	24.00	38.41	50.91	55.97	62.34

^a Ref. [23]

Evans et al. [24]. This torsional frequency differs significantly from our calculated value of 285 cm $^{-1}$.

3.3 Aniline + H system

Reaction energies (ΔE), activation energies (ΔE^\ddagger), reaction standard enthalpies (ΔH), standard enthalpies of activation (ΔH^\ddagger), standard free energies (ΔG), and standard free energies of activation (ΔG^\ddagger) for the five possible channels in aniline + H system are given in Table 2 using BB1 K/6-311 + (2d,p) and G3B3//B3LYP/6-31G(d) levels of theory. Values of ΔE^\ddagger , ΔH^\ddagger , and ΔG^\ddagger calculated with the G3B3 method are within 0.9 kcal/mol from the corresponding values obtained with the BB1 K method. This finding further confirms the comparable performance of BB1 K and the higher level theoretical methods in finding activation barriers for hydrogen atom transfer reactions. Values of ΔE , ΔH , and ΔG calculated with the two theoretical approaches are also in close agreement. All addition channels except that of the *ipso*-site incur noticeable lower energy barriers than the abstraction channel. The calculated reaction barriers for the formation of *o*-($C_6H_5NH_2$)H, *m*-($C_6H_5NH_2$)H, *p*-($C_6H_5NH_2$)H, and *ipso*-($C_6H_5NH_2$)H adducts at the BB1 K/6-311 + (2d,p) are predicted to be 5.0, 5.5, 6.1, and 9.4 kcal mol $^{-1}$, respectively. The abstraction channel is associated with a reaction barrier of 9.5 kcal mol $^{-1}$. As given in Table 2, the formation of *o*-($C_6H_5NH_2$)H, *m*-($C_6H_5NH_2$)H, and *p*-($C_6H_5NH_2$)H is relatively highly exoergic while the formation of the *ipso*-($C_6H_5NH_2$)H adduct and the anilino radical (C_6H_5NH) is modestly exoergic. Optimized geometries for the transition structures are given in Fig. 3. As it is expected, entropic penalty associated with a loss of a molecule during the formation of ($C_6H_5NH_2$)H adducts results in the increase of ΔG and ΔG^\ddagger values in comparison with the corresponding energies and enthalpies values.

The located transition structures (TS1-TS5) are used to derive reaction rate constants within the framework of the TST theory. Modified Arrhenius parameters for the forward and reverse reactions are given in Table 3. Reaction rate constants for the five forward channels are now given in Table 4. As it can be noticed, the contribution from corrections of tunneling is very modest at the temperatures of interest. Based on the rate constants expressions given in Table 3, it is evident that the reaction aniline + H is largely dominated by addition at *ortho*- and *meta* sites at all temperatures. As the temperature increases, the contribution of the abstraction channel becomes more profound due to the entropic effects associated with conserving same number of species in this channel. For instance, the abstraction channel contributes 6, 10, and 13% at 1,000, 1,600 and 2,000 K, respectively.

The calculated reaction rate constant for the abstraction is compared with that for the corresponding experimental values in Fig. 4. Our calculated values reproduce the experimental measurements [8] satisfactorily. The calculated and the experimental values are within factors between 1.13 and 1.20 in the temperature interval (1,000–1,140 K).

The calculated bond dissociation enthalpy of anilino-H at the BB1 K/6-311 + G(2d,p) and G3B3//B3LYP/6-31G(D) levels of theory are 89.5 kcal mol $^{-1}$ and 92.5 kcal mol $^{-1}$, respectively. This value is close to the previously estimated value of 87.9 kcal mol $^{-1}$ [25]. Using the experimental standard enthalpy of formation for H atom (52.1 kcal mol $^{-1}$) [26] and aniline molecule (20.8 ± 0.21 kcal mol $^{-1}$) [26] together with the calculated enthalpy of dissociation of the anilino-H bond, a value of 59.1 kcal mol $^{-1}$ is derived for the standard enthalpy of formation of the anilino radical at 298 K. To the best of our knowledge, there are no other literature values with which to compare our calculated value. The value calculated herein for the dissociation of the anilino-H bond is very close to the well-established corresponding value for phenoxy-H in phenol (89.0 ± 1.0 kcal mol $^{-1}$) [27]. Since the abstraction of H from the amino group in aniline or from the hydroxyl group in phenol depends merely on the bond energy of N–H/OH bond rather than on the steric effect induced by the two functional groups on the phenyl ring, our rate constants for the abstraction channel are compared also with the corresponding experimental values in case of phenol. Our calculated rate constants per H atom abstracted from the amine group at 1,000 K and 1,100 K, respectively, are calculated to be 5.59×10^{-13} and 9.07×10^{-13} cm 3 molecule $^{-1}$ s $^{-1}$, respectively. These values differ by only factors of 1.50 and 1.38, respectively, from the corresponding experimental values [28] of H abstraction from the hydroxyl group in phenol.

Table 2 Reaction energies (ΔE), activation Energies (ΔE^\ddagger), reaction standard enthalpies (ΔH), standard enthalpies of activation (ΔH^\ddagger), standard free energies (ΔG), and standard free energies of activation (ΔG^\ddagger)

Products	ΔE		ΔE^\ddagger		ΔH		ΔH^\ddagger		ΔG		ΔG^\ddagger	
	BB1 K	G3B3	BB1 K	G3B3	BB1 K	G3B3	BB1 K	G3B3	BB1 K	G3B3	BB1 K	G3B3
<i>o</i> -(C ₆ H ₅ NH ₂)H	-24.2	-23.4	5.0	5.0	-25.3	-24.5	3.9	4.0	-18.3	-17.5	11.0	10.9
<i>m</i> -(C ₆ H ₅ NH ₂)H	-21.8	-20.5	5.5	6.4	-22.0	-21.5	5.0	5.4	-15.1	-14.6	12.1	12.4
<i>p</i> -(C ₆ H ₅ NH ₂)H	-20.3	-21.4	6.1	6.0	-22.8	-22.4	4.5	5.0	-16.1	-15.7	11.5	12.0
<i>ipso</i> -(C ₆ H ₅ NH ₂)H	-11.5	-12.2	9.4	9.5	-12.6	-11.8	13.0	8.3	-6.0	-6.4	16.0	15.6
C ₆ H ₅ NH ₂ + H ^a	-12.3	-12.5	9.5	10.4	-12.0	-12.2	8.3	9.3	-23.1	-13.2	15.4	16.3

All values are in kcal mol⁻¹. Values of ΔH , ΔH^\ddagger , ΔG , and ΔG^\ddagger are calculated at 298.15 K

ΔE and ΔE^\ddagger values are corrected with ZPVE

^a Unit of A for the reverse reaction is cm³ molecule⁻¹ s⁻¹

As the *o*-(C₆H₅NH₂)H adduct is predicted to be the most plausible product from the reaction of the aniline molecule with the hydrogen atom as evident from the rate constants given in Table 4, its further rearrangements are investigated. Figure 5 shows the four most probable exit channels for the *o*-(C₆H₅NH₂)H adduct: H migration into *meta*- and *ipso* sites, β C–C bond scission and direct expulsion of hydrogen atom. It is worth mentioning that a transition structure for a concerted elimination of a hydrogen molecule from the -CH₂- and -NH₂ groups could not be located despite numerous attempts. This, in turn, strongly suggests that the sole pathway for the formation of the anilino radical is through abstraction. This finding is in consensus with the satisfactory agreement between the calculated and the experimentally measured rate constants for the abstraction channel.

β C–C bond scission through the transition structure TS8 is found to incur a substantial activation barrier of 60.8 kcal mol⁻¹. This process is predicted to be endoergic by 58.4 kcal mol⁻¹. H transfers forming *m*-(C₆H₅NH₂)H and *ipso*-(C₆H₅NH₂)H adducts are found to require sizable activation barriers of 46.5 and 54.6 kcal mol⁻¹ through transition structures TS6 and TS7, respectively. The most accessible pathway is predicted to be the deactivation of the initial addition channel. Hydrogen expulsion from the *ortho* C atom is found to reform the aniline molecule through an activation barrier of 29.1 kcal mol⁻¹ characterized by the transition structure TS1. Accordingly, the fate of the *o*-(C₆H₅NH₂)H adduct is most likely to be the reverse of the addition channel. This finding is in line with the analysis of He et al. [8] who concluded that the cyclohexadienyl radical formed upon addition is unstable and would immediately undergo the reverse reaction to the initial reactants.

3.4 NH₂ + benzene system

The reaction of the amine group with wide range of hydrocarbons has been thoroughly studied. For instance, Demissy and Lesdaux [29] taken measurements using

laser-resonance absorption to estimate rate constants for NH₂ reaction with methane, ethane, propane, and n-butane in the temperature range 300–520 K. Conversely, reaction rate constants for the reaction of the amine group with aromatic compounds are not available in the literature even for the simplest aromatic compound, benzene, either theoretically or experimentally. To this end, we report in this section theoretical derivation of reaction rate constants for amino radical + benzene.

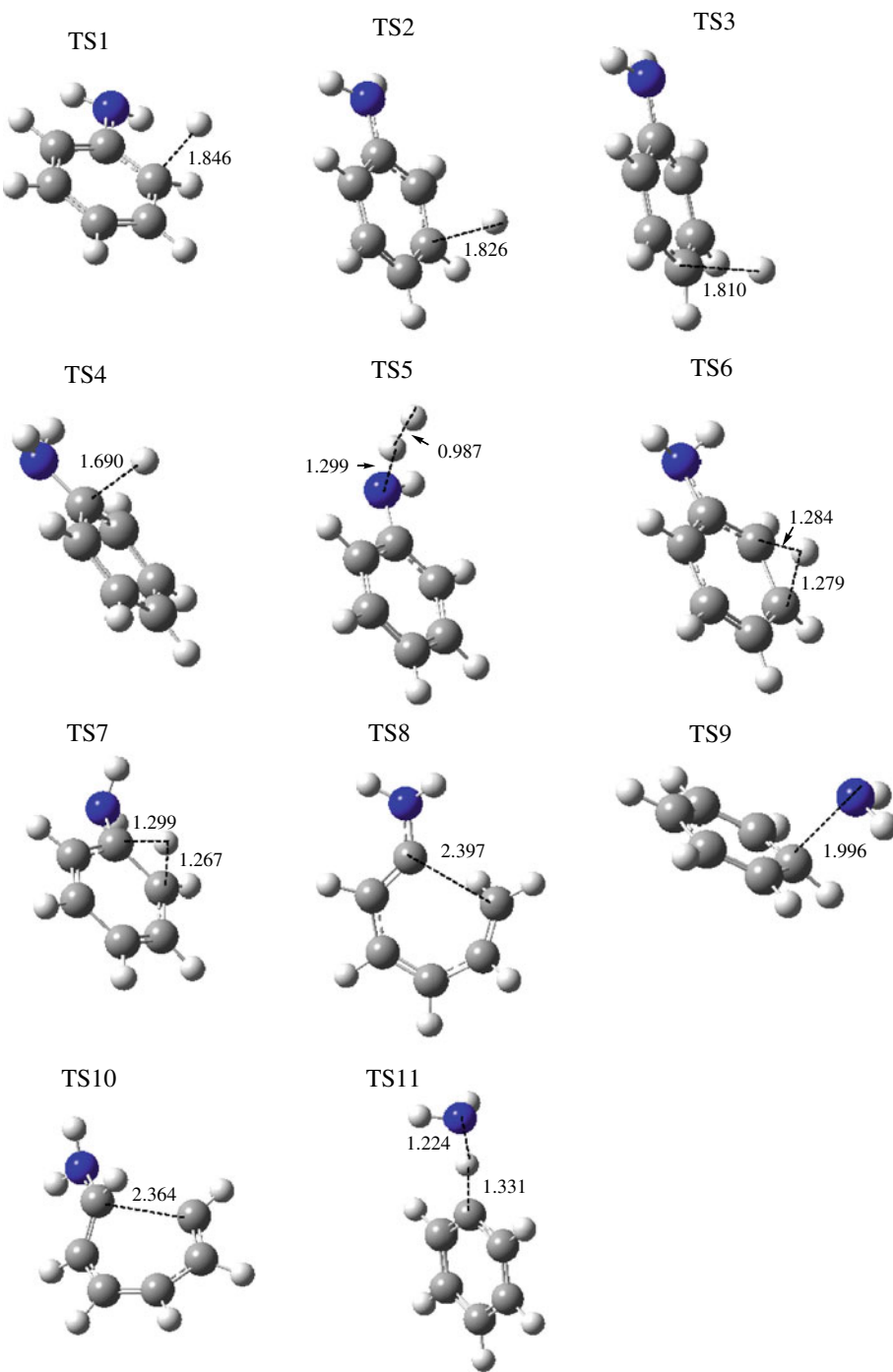
The formation of ammonia (NH₃) and phenyl radical via the abstraction channel is predicted to be slightly endoergic by 3.1 kcal mol⁻¹. This value could be compared with the corresponding experimental enthalpy for the reaction (C₆H₆ + NH₂ → C₆H₅ + NH₃) at 298.15 K, viz, 4.9 kcal mol⁻¹. The abstraction occurs via the transition structure TS11, which resides 14.0 kcal mol⁻¹ above the entrance channel. The barrier for the addition channel (TS9) is higher than that of the abstraction channel by about 1.0 kcal mol⁻¹. The product of the addition channel, namely *ipso*-(C₆H₅NH₂)H, is located 3.5 kcal mol⁻¹ below the separated reactants.

Rate constant parameters for the abstraction and the addition channels in the system (amine + benzene) are given in Table 5. The rate constant for the abstraction channel is found to be faster than the addition channel by about two order of magnitude at all temperatures. Abstraction/addition behavior of (amino radical + benzene) is different from that of (OH + benzene) [30] where addition dominates at temperatures as high as 400 K whereas in the system of (HO₂ + benzene) [31], the abstraction channel is negligible even at elevated temperatures.

3.5 Amino group displacement

Figure 6 shows the four possible decomposition pathways for the *ipso*-(C₆H₅NH₂)H adduct. Based on the calculated high activation energies, β C–C bond scission and H transfer to the *meta* position are expected to be of

Fig. 3 Optimized structures for transition states. Interatomic distances are in Å



negligible importance. The fate of the *ipso*-(C₆H₅NH₂)H is either to form an aniline molecule via H expulsion or to form a benzene molecule through the expulsion of the amino group.

The analogous systems of *ipso*-(C₆H₅CH₃)H and *ipso*-(C₆H₅OH)H are expected to exhibit similar features with regard to the relative importance of benzene formation and the expulsion of the functional group over the other two channels, i.e., β C–C bond scission and H transfer to the

metaposition. In their studies, He et al., found that NH₂ displacement in aniline proceeded at a similar rate to OH or CH₃ displacement from phenol and toluene, respectively. To probe the validity of their finding, we report in Table 6 our calculated reaction energy and activation barrier for the formation of an *ipso*-cyclohexadienyl-type radical upon the *ipso* addition of H atom to phenol and toluene. Results are compared with the corresponding results for aniline. As expected, the methyl electron-donating group results in

Table 3 Modified Arrhenius parameters for the five channels in the reaction $\text{C}_6\text{H}_5\text{NH}_2 + \text{H}$

Products	$A(\text{f})$	$n(\text{f})$	$Ea(\text{f})/R$	$A(\text{r})$	$n(\text{r})$	$Ea(\text{r})/R$
<i>o</i> -($\text{C}_6\text{H}_5\text{NH}_2$)H	1.23×10^{-15}	1.55	1,800	1.1×10^{10}	1.10	14,500
<i>m</i> -($\text{C}_6\text{H}_5\text{NH}_2$)H	7.08×10^{-16}	1.62	2,200	6.0×10^{19}	1.16	15,000
<i>p</i> -($\text{C}_6\text{H}_5\text{NH}_2$)H	4.71×10^{-16}	1.58	2,000	5.0×10^9	1.10	13,500
<i>ipso</i> -($\text{C}_6\text{H}_5\text{NH}_2$)H	6.29×10^{-17}	1.74	6,000	6.2×10^8	1.29	9,900
$\text{C}_6\text{H}_5\text{NH} + \text{H}_2^{\text{a}}$	5.08×10^{-14}	1.08	4,200	4.8×10^{-19}	2.08	9,900

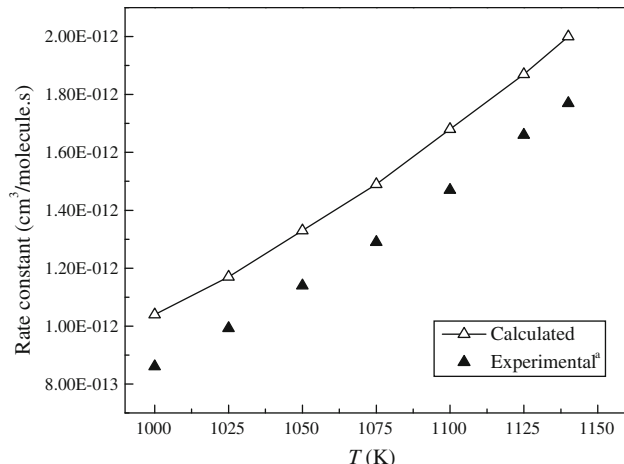
Forward (*f*) (A in $\text{cm}^3 \text{molecule}^{-1} \text{s}^{-1}$ and $Ea(\text{f})/R$ in K) and reverse (*r*) (s^{-1}) and $Ea(\text{r})/R$ in K. Values are fitted in the temperature range of 300 K to 2000 K

^a Unit of A for the reverse reaction is $\text{cm}^3 \text{molecule}^{-1} \text{s}^{-1}$

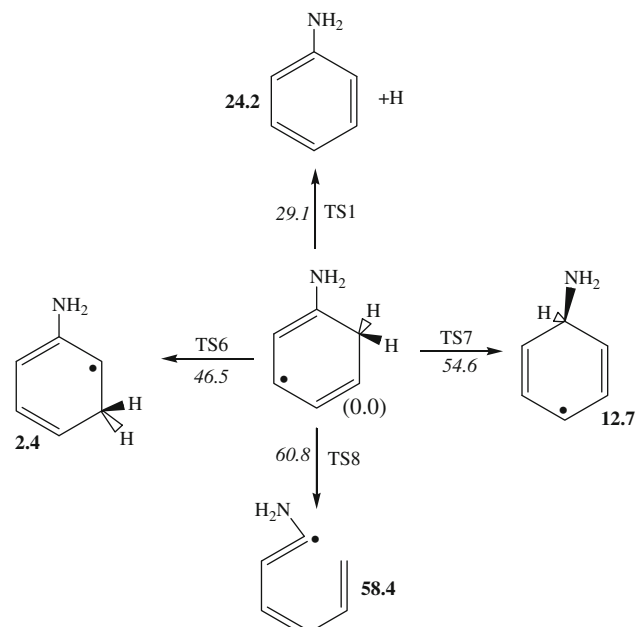
Table 4 Calculated forward rate constants for the five channels in the reaction $\text{C}_6\text{H}_5\text{NH}_2 + \text{H}$

T (K)	<i>o</i> -($\text{C}_6\text{H}_5\text{NH}_2$)H	<i>m</i> -($\text{C}_6\text{H}_5\text{NH}_2$)H	<i>p</i> -($\text{C}_6\text{H}_5\text{NH}_2$)H	<i>ipso</i> -($\text{C}_6\text{H}_5\text{NH}_2$)H	$\text{C}_6\text{H}_5\text{NH} + \text{H}_2$
300	2.35E-14 (2.10)	4.21E-15 (2.53)	4.87E-15 (2.33)	3.192E-21 (4.12)	2.879E-16 (50.34)
400	1.58E-13 (1.61)	4.14E-14 (1.78)	3.95E-14 (1.70)	6.798E-19 (2.23)	2.501E-15 (7.81)
600	1.32E-12 (1.31)	5.21E-13 (1.38)	4.03E-13 (1.35)	2.054E-16 (1.52)	5.146E-14 (2.57)
800	4.39E-12 (1.21)	2.13E-12 (1.25)	1.48E-12 (1.23)	4.177E-15 (1.33)	3.238E-13 (1.81)
1,000	9.75E-12 (1.16)	5.38E-12 (1.18)	3.50E-12 (1.17)	2.761E-14 (1.24)	1.117E-12 (1.54)
1,200	1.74E-11 (1.12)	1.05E-11 (1.15)	6.54E-12 (1.14)	1.024E-13 (1.18)	2.760E-12 (1.40)
1,400	2.74E-11 (1.10)	1.75E-11 (1.12)	1.06E-11 (1.11)	2.708E-13 (1.15)	5.552E-12 (1.32)
1,600	3.96E-11 (1.09)	2.65E-11 (1.10)	1.56E-11 (1.10)	5.772E-13 (1.13)	9.736E-12 (1.26)
1,800	5.37E-11 (1.08)	3.74E-11 (1.09)	2.16E-11 (1.08)	1.062E-12 (1.11)	1.550E-11 (1.22)
2,000	6.98E-11 (1.07)	5.00E-11 (1.08)	2.84E-11 (1.07)	1.758E-12 (1.10)	2.296E-11 (1.19)

Values in brackets are the estimated corrections for tunneling. Values are in $\text{cm}^3 \text{molecule}^{-1} \text{s}^{-1}$

**Fig. 4** Comparison between the calculated and experimental reaction rate constants for the reaction $\text{C}_6\text{H}_5\text{NH}_2 + \text{H} \rightarrow \text{C}_6\text{H}_5\text{NH} + \text{H}_2$.

^aRef. [8]

**Fig. 5** Reaction scheme for the unimolecular rearrangements of *o*-($\text{C}_6\text{H}_5\text{NH}_2$)H. Values in bold are the reaction energies, and values in italics are the activation barriers: both calculated at 0 K. Energies in kcal mol⁻¹

more stability of the *ipso*-($\text{C}_6\text{H}_5\text{CH}_3$)H adduct when comparing *ipso*-($\text{C}_6\text{H}_5\text{OH}$)H and *ipso*-($\text{C}_6\text{H}_5\text{NH}_2$)H adducts.

Table 5 Modified Arrhenius parameters the two reactions $C_6H_6 + NH_2 \rightarrow ipso-(C_6H_5NH_2)H$ and $C_6H_6 + NH_2 \rightarrow C_6H_6 + NH_3$

Reaction	$A(f)$	$n(f)$	$Ea(f)/R$	$A(r)$	$n(r)$	$Ea(r)/R$
$C_6H_6 + NH_2 \rightarrow ipso-(C_6H_5NH_2)H$	8.32×10^{-19}	1.76	6,700	5.13×10^{14}	-0.66	9,700
$C_6H_6 + NH_2 \rightarrow C_6H_6 + NH_3$	1.23×10^{-21}	3.28	6,300	3.25×10^{-22}	3.10	4,000

All units are given in Table 2. Values are fitted in the temperature range of 300 K to 2,000 K

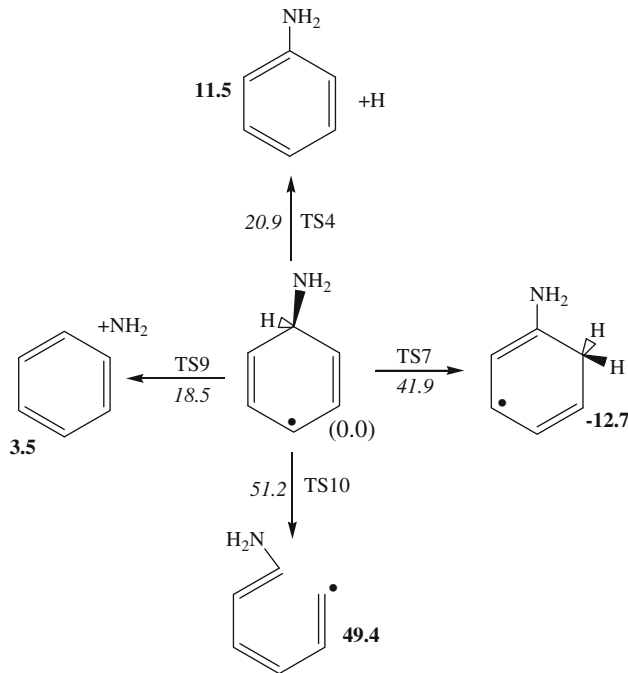


Fig. 6 Reaction scheme for the unimolecular rearrangements of *ipso*-($C_6H_5NH_2)H$. Values in bold are the reaction energies, and values in italic are the activation barriers: both calculated at 0 K. Energies in kcal mol⁻¹

Here, we investigate the formation of benzene in these three systems based on the reaction scheme:

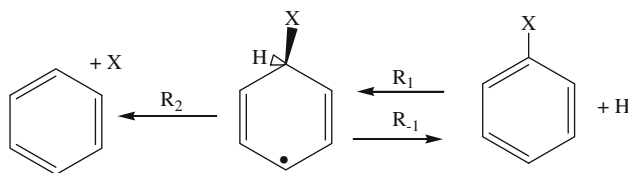


Table 6 Reaction (ΔE) and activation ($\Delta E''$) energies for the three reactions involved in *ipso*-addition channels in toluene, phenol, and aniline (R_1 , R_2 and R_{-1})

X	ΔE			$\Delta E''$			A			n			Ea/R		
	NH ₂	CH ₃	OH	NH ₂	CH ₃	OH	NH ₂	CH ₃	OH	NH ₂	CH ₃	OH	NH ₂	CH ₃	OH
R ₁	-11.5	-18.9	-14.1	9.4	7.5	9.6	4.75×10^{-11}	5.29×10^{-17}	7.36×10^{-17}	0.0	1.64	1.76	4,700	2,800	3,700
R ₋₁	11.5	18.9	14.1	20.9	26.4	23.7	6.24×10^8	1.15×10^{12}	5.54×10^{12}	1.29	0.61	0.25	9,900	11,800	7,900
R ₂	3.5	9.8	12.4	18.5	22.9	15.2	5.16×10^{14}	5.00×10^9	7.90×10^8	-0.66	1.14	1.27	9,700	13,000	11,300

All units are given in Table 2. Reaction rate parameters are fitted in the temperature range of 300 K to 2,000 K

Table 6 gives Arrhenius parameters for the three reactions R_1 , R_{-1} , and R_2 for the three systems of aniline, toluene, and phenol. The branching ratios for benzene formation, i.e., $k_2/(k_2 + k_{-1})$ are given in Fig. 7 in Table 7 for the three systems. Over the temperature range of 1,000–1,140 K at which the experimental study is conducted, the yield of benzene from the *ipso* adducts amount to 94–95%, 99–100%, and 54–63%, respectively, in systems of toluene, phenol, and aniline, respectively. Virtually, each hydrogen addition at an *ipso* site leads to displacement of the methyl and hydroxyl groups in systems of toluene and phenol, respectively. Consequently, the reaction rate constant for H addition at the *ipso* site in toluene and phenol as given in Table 4 (R_1) can be considered to be an upper limit for the rate constant for $H + C_6H_5CH_3 \rightarrow C_6H_6 + CH_3$ and $H + C_6H_5OH \rightarrow C_6H_6 + OH$.

In Figs. 8 and 9, our calculated rate constants for methyl and hydroxyl displacement by H atom in toluene and phenol, respectively, are compared with the available experimental results for these two reactions. The calculated and the experimental rate constants for these two reactions are in relatively close agreement. For instance, the calculated rate constants for hydroxyl displacement in case of phenol are within a factor 2.0 of the corresponding experimental values [28]. For toluene, the calculated rate constants for methyl group displacement differ from the two sets of corresponding experimental values [32, 33] by factors of 2.0–5.0.

In case of aniline, the reaction rate constant for the amine group displacement and the formation of benzene ($C_6H_5NH_2 + H \rightarrow C_6H_6 + NH_2$) is calculated as $k_2/(k_2 + k_{-1}) \times k_1$ and the obtained rate constant is fitted to modified Arrhenius parameters as $1.49 \times 10^{-11} \exp(-4,200/T) \text{ cm}^3 \text{ molecule}^{-1} \text{ s}^{-1}$. Figure 10 shows the

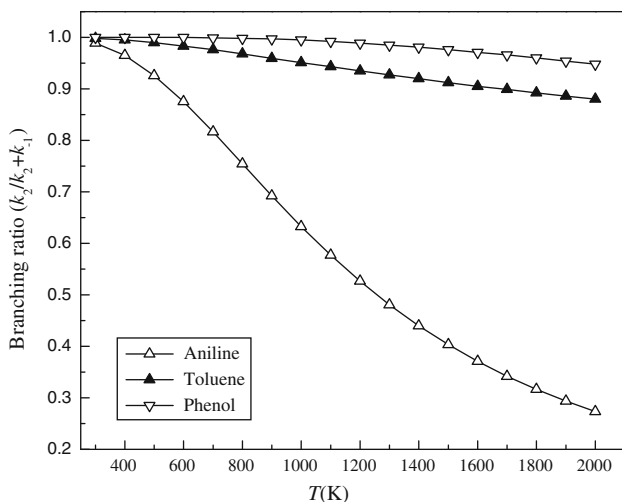


Fig. 7 Branching ratio of $k_2/(k_2 + k_{-1})$ for aniline, toluene, and phenol systems

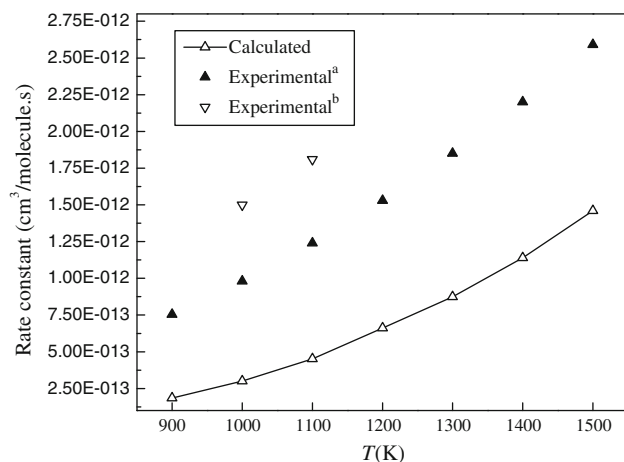


Fig. 8 Comparison between the calculated and experimental reaction rate constants for the reaction $\text{H} + \text{C}_6\text{H}_5\text{CH}_3 \rightarrow \text{C}_6\text{H}_6 + \text{CH}_3$. ^aRef. [33], ^bRef. [32]

Table 7 Calculated rate constants for reaction R₋₁ and R₂ and the branching ratio for benzene formation, i.e., $(k_2/(k_2 + k_{-1}))$ in the systems of aniline, toluene, and phenol

Aniline			Toluene			Phenol			
k_{-1}	k_2	$k_2/(k_2 + k_{-1})$	k_{-1}	k_2	$k_2/(k_2 + k_{-1})$	k_{-1}	k_2	$k_2/(k_2 + k_{-1})$	
300	1.14E-03	1.01E-01	9.89E-01	5.28E-07	3.43E-04	9.98E-01	4.73E-05	8.78E+01	1.00E+00
400	9.72E+00	2.67E+02	9.65E-01	3.32E-02	6.84E+00	9.95E-01	7.32E-01	6.55E+04	1.00E+00
600	9.68E+04	6.78E+05	8.75E-01	2.75E+03	1.62E+05	9.83E-01	1.60E+04	5.30E+07	1.00E+00
800	1.07E+07	3.27E+07	7.54E-01	8.99E+05	2.69E+07	9.68E-01	2.72E+06	1.56E+09	9.98E-01
1,000	1.88E+08	3.24E+08	6.33E-01	3.06E+07	5.97E+08	9.51E-01	6.28E+07	1.20E+10	9.95E-01
1,200	1.31E+09	1.45E+09	5.26E-01	3.31E+08	4.76E+09	9.35E-01	5.24E+08	4.72E+10	9.89E-01
1,400	5.30E+09	4.15E+09	4.40E-01	1.84E+09	2.11E+10	9.20E-01	2.43E+09	1.25E+11	9.81E-01
1,600	1.53E+10	8.99E+09	3.71E-01	6.74E+09	6.45E+10	9.05E-01	7.75E+09	2.61E+11	9.71E-01
1,800	3.50E+10	1.62E+10	3.16E-01	1.86E+10	1.54E+11	8.92E-01	1.92E+10	4.61E+11	9.60E-01
2,000	6.81E+10	2.56E+10	2.73E-01	4.20E+10	3.09E+11	8.80E-01	3.99E+10	7.27E+11	9.48E-01

comparison between our calculated reaction rate constant and the available experimental results. The calculated values for these reaction rate constants are consistently lower than the corresponding experimental values by a factor of 3.0.

Based on the energetics trend for the three systems given in Table 6 and the satisfactory agreement between the experimental and the calculated rate constants for displacement channels in aniline, phenol, and toluene, our findings agree with the conclusions of He et al. [8] that all three systems have comparable rate constants for benzene generation via displacement. It is worthwhile mentioning that the pattern and degree of chlorination on the aniline ring are more likely to exhibit noticeable change in the

reaction of chlorinated aniline isomers with hydrogen in an analogy to chlorinated phenol + H system [34–36].

4 Conclusions

Reaction and activation energies for ($\text{H} + \text{aniline}$) and ($\text{NH}_2 + \text{benzene}$) systems are obtained. The heat of formation of the resonance stabilized anilino radical is found to be 59.1 kcal mol⁻¹. The reaction $\text{NH}_2 + \text{benzene}$ is found to branch predominantly into $\text{NH}_3 + \text{C}_6\text{H}_5$ even at low temperatures, and the addition channel is of negligible importance. Based on the calculated activation energies and rate constants, amino group displacement from the aniline

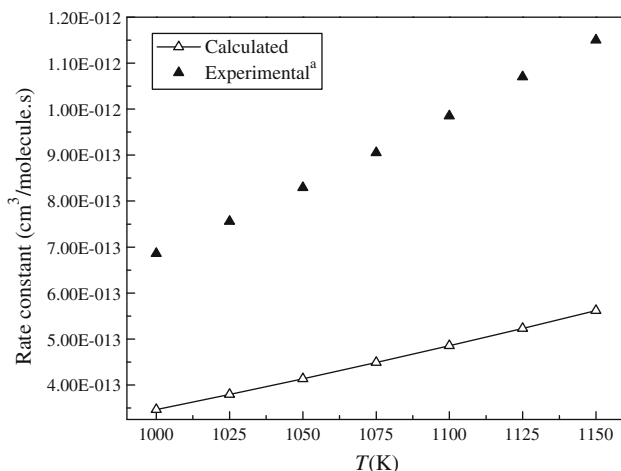


Fig. 9 Comparison between the calculated and experimental reaction rate constants for the reaction $\text{H} + \text{C}_6\text{H}_5\text{OH} \rightarrow \text{C}_6\text{H}_6 + \text{OH}$. ^aRef. [28]

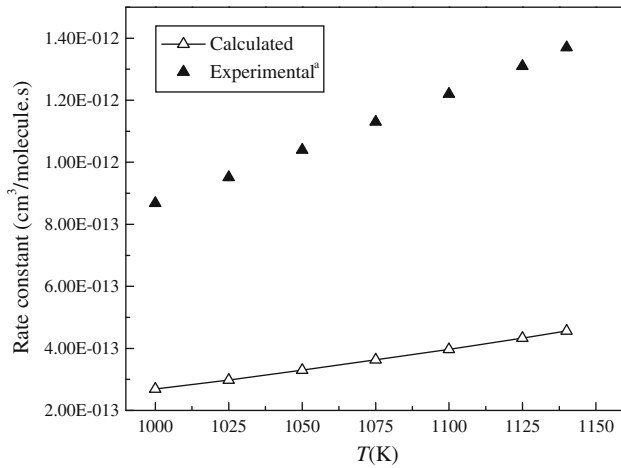


Fig. 10 Comparison between the calculated and experimental reaction rate constants for the reaction $\text{H} + \text{C}_6\text{H}_5\text{NH}_2 \rightarrow \text{C}_6\text{H}_6 + \text{NH}_2$. ^aRef. [28]

molecule upon H addition at the *ipso* position is shown to be significantly slower than the corresponding displacements in toluene and phenol of methyl and hydroxyl. Overall, H reaction with aniline is found to produce the anilino radical and benzene in comparable rates.

Acknowledgments This study has been supported by a grant of computing time from the Australian Centre of Advanced Computing and Communications (ac3).

References

- Aniline Fact Sheet (CAS No. 62-53-3) (1994) Pollution prevention and toxics. Washington, DC
- Jones CR, Liu Y-Y, Sepai O, Yan H, Sabbioni G (2005) Environ Sci Technol 40:387
- Calaf RE, Pena J, Paytubi S, Blount BC, Posada de la Paz M, Gelpi E, Abian J (2001) Anal Chem 73:3828
- Ferge T, Maguhn J, Hafner K, Muhlberger F, Davidovic M, Warnecke R, Zimmermann R (2005) Environ Sci Technol 39:1393
- Atkinson R, Tuazon EC, Wallington TJ, Aschmann SM, Arey J, Winer AM, Pitts JN (1987) Environ Sci Technol 21:64
- Patil SS, Shinde VM (1988) Environ Sci Technol 22:1160
- Yang K, Wu W, Jing Q, Zhu L (2008) Environ Sci Technol 42:7931
- He YZ, Cui JP, Mallard WG, Tsang WJ (1988) J Phys Chem 92:1510
- Frisch MJT, Trucks GW, Schlegel HB, Scuseria GE, Robb MA, Cheeseman JR, Zakrzewski VG, Montgomery JA, Stratmann RE, Burant JC, Dapprich S, Millam JM, Daniels RE, Kudin KN, Strain MC, Farkas O, Tomasi J, Barone VCM, Cammi R, Mennucci B, Pomelli C, Adamo C, Clifford S, Ochterski J, Petersson GA, Ayala PY, Cui Q, Morokuma K, Salvador P, Dannenberg JJ, Malick DK, Rabuck AD, Raghavachari K, Foresman JB, Cioslowski JO, Baboul AG, Stefanov BB, Liu G, Liashenko A, Piskorz P, Komaromi I, Gomperts R, Martin RL, Fox DJ, Keith T, Al-Laham MA, Peng CY, Nanayakkara A, Challacombe M, Gill PMW, Johnson B, Chen W, Wong MW, Andres JL, Gonzalez CM, Head-Gordon M, Replogle ES, Pople JA (2001) Gaussian 03; revision A. 11th edn. Gaussian, Inc, Pittsburgh
- Zhao Y, Lynch BJ, Truhlar DGJ (2004) Phys Chem A 108:2715
- Montgomery JA, Ochterski JW, Petersson GA (1994) J Chem Phys 101:5900
- Kohn W, Sham LJ (1965) Phys Rev A 140:1133
- Zhao Y, Gonzalez-Garcia N, Truhlar DG (2005) J Phys Chem A 109:2012
- McClurg RB, Flagan RC, Goddard WA (1997) J Chem Phys 106:6675
- Mokrushin V, Bedanov V, Tsang W, Zachariah M, Knyazev V (2002) ChemRate; version 1, 19th edn. NIST, Gaithersburg
- Eyring HJ (1935) Chem Phys 3:107
- Eckart C (1930) Phys Rev 35:1303
- Duncan WT, Bell RL, Truong TN (1998) J Comput Chem 19:1309
- Fukuyo M, Hirotsu K, Higuchi T (1982) Acta Cryst B 38:640
- Alcolea Palafox M, Meléndez F (1999) J Mol Struct: THEOCHEM 493:171
- Larsen NW, Hansen EL, Nicolaisen FM (1976) Chem Phys Lett 43:584
- Halpern RM, Ramachandran BR, Glendening ED (2007) J Chem Edu 84:1067
- Hussein AP, Lielmezs J, Aleman H (1985) Thermochimica Acta 86:209
- Evans JC (1960) Spectrochim Acta 42B
- Michael JV, Sutherland JW, Klemm RJ (1986) Phys Chem 90:497
- Good WD, Smith NK (1969) J Chem Eng Data 14:102
- da Silva G, Chen C-C, Bozzelli JW (2006) Chem Phys Lett 424:42
- He YZ, Mallard WG, Tsang W (1988) J Phys Chem 92:2196
- Demissy M, Lesclaux R (1980) J Am Chem Soc 102:2897
- Zhu L, Bozzelli JW (2003) J Phys Chem A 107:3696
- Altarawneh M, Dlugogorski BZ, Kennedy EM, Mackie JC (2010) Combust Flame 157:1325
- Robaugh D, Tsang WJ (1988) J Phys Chem 80:4159
- Ellis C, Scott MS, Walker RW (2003) Combust Flame 132:291
- Zhang QZ, Qu XH, Xu F, Shi XY, Wang WX (2009) Environ Sci Technol 43:4105
- Li S, Zhang Q, Wang W (2006) Chem Phys Lett 428:262
- Xu F, Wang H, Zhang QZ, Zhang RX, Qu XH, Wang WX (2010) Environ Sci Technol 44:1399